X-645-72-216

PREPRINT

POLAR CAP ELECTRIC FIELD DISTRIBUTIONS RELATED TO THE INTERPLANETARY MAGNETIC FIELD DIRECTION

J. P. HEPPNER

JUNE 1972

GSFC

GODDARD SPACE FLIGHT CENTER

GREENBELT, MARYLAND

Polar Cap Electric Field Distributions related to the Interplanetary Magnetic Field Direction

J. P. Heppner
NASA Goddard Space Flight Center
Greenbelt, Maryland

June 1972

"Letter" for publication in the Journal of Geophysical Research

Polar Cap Electric Field Distributions related to the Interplanetary Magnetic Field Direction

J. P. Heppner

NASA Goddard Space Flight Center
Greenbelt, Maryland

In a previous paper (Heppner, 1972a) measurements of the electric field taken by OGO-6 throughout a 13 day period (June 10-22, 1969) when the orbit plane was centered on the 18^h-6^h local time meridian were described with emphasis on the stability of the basic high latitude electric field pattern. The term "pattern" implies the direction of the electric field as a function of location in magnetic time (MLT) and invariant latitude (Λ) coordinates. In essence it was shown that at auroral belt latitudes in both hemispheres the electric field is consistently directed poleward in the mid-evening sector and equatorward in the mid-morning sector (i.e., from dusk toward dawn) whereas the field at higher, polar cap, latitudes is consistently directed from dawn toward dusk. By consistently, one means independent of magnetic disturbance conditions, interplanetary field directions, and other parameters that might be expected to have some relationship to the electric field pattern. The continuous existence of a sequence of signs as a function of latitude does not however mean that there are not substantial variations in magnitudes and the latitudes where the sign reverses between auroral belt and polar cap directions. Also, multiple sign reversals are often encountered near the transition (or boundary) between auroral belt and polar cap fields. Examples are given in Heppner (1972a) and discussed further relative to complementary information provided by barium ion cloud experiments in Heppner (1972b).

Figure 1, which shows data from successive passes over southern and northern high latitudes, is chosen to illustrate how grossly asymmetric the distribution

of magnitudes can sometimes be, and also to provide an example of the anti-correlation between southern and northern polar cap magnitude distributions discussed later. The anti-correlation to note in Figure 1 is the existence of maximum, dawn-dusk directed, polar cap field adjacent to the evening auroral belt in the southern hemisphere but adjacent to the morning auroral belt in the northern hemisphere. The two northern hemisphere passes in Figure 1 also illustrate one of a number of characteristic field distributions observed in the northern polar cap; that is, in crossing the polar cap from evening toward morning, $|E_x|$ increases almost linearly until near the morning auroral belt where a rapid decrease in $|E_x|$ occurs and the sign reverses.

Signature Classification

The fact that different characteristic distributions of the polar cap field reappeared on different days and at a variety of UT times throughout the 13 days, led to the idea that one could classify the distributions in terms of "signatures" which could then be compared with other geophysical parameters with the hope that correlations might appear which would suggest an explanation for the changes in distribution. After several trial examinations it was apparent that for roughly two-thirds of the northern hemisphere traverses the polar cap distributions could be identified in terms of the "signatures" shown in Figure 2. For the other one-third one could only use combinations of the Figure 2 signatures or end up with an unreasonable number of signatures. These cases are thus omitted from the statistics given later. Also passes intersecting the noon-midnight meridian at $\Lambda < 75^\circ$ on the nightside are omitted because the polar cap cross-section at these latitudes becomes too small to regard as being representative. The northern hemisphere signatures are thus only applied to passes crossing the noon-midnight meridian

between $\Lambda = 75^{\circ}$ on the nightside and $\Lambda = 85^{\circ}$ on the dayside. For the southern polar cap, noon-midnight meridian crossings extend from about $\Lambda = 70^{\circ}$ on the dayside to $\Lambda = 85^{\circ}$ on the nightside. As the electric field in the dayside region between 70° and 80°, and frequently 70° to 85°, is characteristically highly irregular with many sign reversals, classification of the southern polar cap field is generally limited to traverses crossing between $\Lambda = 85^{\circ}$ on the dayside and $\Lambda = 85^{\circ}$ on the nightside. A further complication in the southern polar cap is that irregularities are usually more prominent than in the northern polar cap even when the southern polar cap crossing is on the nightside (see Heppner, 1972a). Thus the number of southern polar cap traverses that can be classified is considerably less than in the northern polar cap and for meaningful statistics it becomes necessary to characterize the field in broader categories than the signatures used in the northern polar cap, as noted later.

The fact that correlations between the azimuthal direction of the interplanetary magnetic field and the most simple polar cap signatures were immediately obvious is the basis of this communication. Because of their potential importance the simple correlations are presented here to make the information available at an early date. Thus, here we will omit the more complex signatures (F,G,H,I and K) for discussion at a later date when more comprehensive analyses can be completed. These analyses involve use of different coordinate systems, testing correlations as a function of time differences between interplanetary and polar cap observations, and looking for statistical correlations between interplanetary parameters and more detailed features such as the sharpness and location of polar cap-auroral belt boundaries, the existence of multiple field reversals, large differences between magnitudes in morning and evening auroral belt regions, etc.

In the present analysis the distribution of fields within auroral belt (i.e., sunward convection) regions is ignored and only the spatial distribution of the dawn-dusk polar cap field is considered. Thus in Figure 2 all auroral belt distributions are identically drawn except for the signatures SC and RC. These are included in the present analysis because their correlation with the interplanetary magnetic field so closely resembles that of signatures B and C.

Correlations

For each traverse across the northern or southern polar cap the simultaneous values of the interplanetary (IP) magnetic field in solar-equatorial coordinates from the Ames magnetometer on Explorer-33 were recorded in terms of 4γ buckets for the magnitude (B), eight angle sectors for the longitudinal angle (ϕ), and six angle sectors for the latitudinal angle (θ). Values were then grouped for each electric field signature and plotted as histograms. When the interplanetary magnetic field was changing between the times OGO-6 entered and left the polar cap such that values fell into more than one magnitude bucket or angle sector during this time interval, typically between 6 and 12 minutes, fractional occurrences were tabulated (e.g., if ϕ changed from 80° to 170° an occurrence of one-third was listed for each of the 3 sectors of ϕ in which measurements fell).

Figure 3 shows the resulting IP field histograms for the 28 (A) cases in which the electric field had an unambiguous "flat" magnitude distribution across the northern polar cap. ϕ angles of 270°-360° were obviously most prevalent at these times. There does not appear to be any selectivity in the θ angle or the magnitude $|B|$ relative to average conditions. The 3-hour Kp values that accompanied these cases are also shown; they are relatively random. Cases in which the northern polar cap electric field had a pronounced intensity maximum

only in the evening (i.e., D and E signatures) are also shown. As unambiguous, northern polar cap D and E signatures were too rare to treat separately they have been grouped and shown with the A cases because of the similarity in the ϕ distribution. Occurrences between $\phi = 180^{\circ}$ and 225° constitute an apparent exception; however, relative to physical relationships discussed later this is not an exception if the important parameter is the sign of the Y-component rather than "toward" or "away" sectors of the IP field (i.e., analogous to findings of Friis-Christensen et al., 1972). The distributions in θ, B, and Kp for the D and E cases do not suggest correlations of statistical significance.

Figure 4 shows histograms for times when the electric field had a pronounced maximum intensity only on the morning side of the polar cap (i.e., signatures B, C, and SC and RC). In contrast to Figure 3 the distribution in ϕ is almost completely in the 90° to 180° quadrant. However, like Figure 3 there is very little selectivity in the θ angle and in particular the θ distributions for signatures A (Figure 3) and B (Figure 4) are highly similar. However, when the Figure 4 θ distributions are examined in the sequence B to C to SC and RC there is a statistical shift which might have some second order significance. Some tendency for a shift toward lower Kp values also appears.

Figure 5 shows histograms for both cases of evening and morning maximums in the southern polar cap electric field. In terms of the northern polar cap electric field signatures the evening and morning maximum cases are equivalent to the D and E signatures and the B and C signatures, respectively. The contrast in ϕ distributions between cases of evening and morning maximums is very clear. It is also clear that the ϕ distributions are reversed 180° from the equivalent northern polar cap signatures (Note: because signs are reversed in the two hemispheres in spacecraft coordinates and the south polar traverses are from

morning toward evening, a pictorial comparison of northern and southern signatures requires reversals both in sign and left to right sequence). As in the northern hemisphere cases, the θ, $|B|$, and Kp distributions in Figure 5 indicate only the possibility of secondary significance.

To illustrate the anti-correlation of southern and northern polar cap distributions, composite ϕ histograms for the northern polar cap signatures A, D, E and B, C, SC, RC are fhown in Figure 6. 118 polar traverses are thus represented. Except for the (A) cases, flat distribution, the composite signatures are representative only in terms of the location of a pronounced maximum in magnitudes. To date, analyses have not revealed any obvious reasons for why the flat, (A), signatures in the northern hemisphere fit into the correlations essentially the same as cases of evening maximum. Unfortunately practically all "flat" distributions, observed in the southern polar cap (i.e., analogous to A in the northern polar cap) are to various degrees ambiguous as a consequence of regions of superimposed irregularities. Grouping the questionable (A) cases in the southern polar cap gives histograms that are relatively random. Thus, they do not suggest an explanation for the correlative grouping of (A) with (D) and (E) in the northern polar cap.

Discussion

The high degree of correlation with the ϕ angle, apparently independent of other parameters, indicates that the relative geometry of IP and magnetospheric magnetic fields must be fundamental to explaining the distribution of polar cap electric fields. Figure 7, drawn for one orientation of the interplanetary field and the simultaneous distributions of convective velocity in the two polar caps, illustrates the relationship. That is, fast convection occurs on the side (dawn or dusk) where magnetospheric magnetic field lines inside the magnetopause

have a component parallel to the direction of the IP magnetic field; conversely, slow convection occurs on the side where the two magnetic fields have an anti-parallel component. This holds true in both hemispheres and for the reverse direction of the IP field with the qualification, noted previously, that the flat, (A), distributions in the northern polar cap have approximately the same correlation characteristics as cases with an evening maximum in the northern polar cap.

The above statements contain the implication that the sign of the solar-equatorial Y component (perpendicular to the sun-earth line) is a more critical parameter than the sign of the X component (+X towards the sun). This was initially assumed by the author on the basis of more detailed considerations of individual cases which, however, lack statistical significance. The cases with ϕ between 180° and 225° for (D) and (E) signatures in Figure 3 provided one of several types of examples. The assumption is given further credence in terms of the Friis-Christensen, et al. (1972) finding that it is the interplanetary Y component that produces the ϕ angle correlation with dayside polar cap magnetic disturbances found by Svalgaard (1968) and Mansurov (1969). Inasmuch as the present findings provide a rather straightforward explanation for the Svalgaard-Mansurov correlations, the Y component should have a related significance in both analyses.

Because the Svalgaard-Mansurov correlation is an important consequence of the ϕ angle dependence of the polar cap electric field distribution we will digress briefly to illustrate the explanation. In Figure 8 the relationships they found between ϕ and the surface magnetic vectors are shown for northern high latitudes. An idealized average convection pattern for the dayside is shown in the center of the figure. This idealization is justified not only in

terms of many past analyses but also in terms of an analysis of OGO-6 data by Aggson and Bohse (1972) which showed that a relatively symmetric and simple two-cell configuration, similar in principal to that drawn by Axford and Hines (1961), appears when many traverses from both northern and southern hemispheres are grouped and averaged. To the left and right in Figure 8 asymmetrical distributions of the equipotentials (i.e., flow lines) are drawn compatible with the ϕ angle correlations. In addition to the flow asymmetries there is an additive effect from boundary shifts accompanying the asymmetric flow. This comes from numerous observations that the polar cap-auroral belt boundary on the side where the flow is weak usually shifts toward the pole relative to its average position. To at least partially include this effect in Figure 8, the boundary has been shifted about 3° in latitude in the dawn-dusk direction in opposite directions in the left and right patterns. In many cases the shift is considerably greater as indicated by the examples of Figure 1. A consequence of both the asymmetric flow and the boundary shift is that the mid-day convection has continuity with either the morning auroral belt (left) or the evening auroral belt (right) as a function of the ϕ angle of the interplanetary field. The corresponding signs for the magnetic disturbance, at points A and P in Figure 8, are exactly what is expected for ionospheric Hall currents accompanying the convection. Construction of similar diagrams for the anti-correlated distributions in the southern polar cap, relative to the same ϕ angles, readily shows that this explanation also gives the proper signs for the simultaneous magnetic changes observed at southern high latitudes by Svalgaard (1968) and Mansurov (1969). Thus the Svalgaard-Mansurov correlations are a logical consequence of the polar cap electric field distributions. In view of the observation that these distributions do not appear to be directly related to the θ component, there is not an

obvious basis for explanation in terms of field line merging (Wilhjelm and Friis-Christensen, 1972; Jorgensen et al., 1972) unless a more comprehensive theory for explaining the electric field distributions can be developed along such lines.

The correspondence between fast convection and parallel magnetospheric and interplanetary magnetic fields, noted above, indicates the need for more critical theory in relating magnetospheric convection to external interplanetary conditions. Certainly there is little in common between these observations and simple predictions based on field line merging mechanisms. In terms of viscous interaction near the magnetopause the observations are not conflicting but mechanisms which relate the viscosity, or drag, to relative field orientations are lacking; these should be vigorously sought. It is not apparent that the problem is strictly one of local momentum transfer in that the observations relate only a velocity, $\underline{v}$, and not necessarily mass, m, to the interplanetary field. Along these lines it should also be recognized that the correlations between polar cap electric field distributions and the interplanetary magnetic field presented here, do not suggest any direct relationship with particle entry into, or acceleration within, the magnetosphere; particularly in view of the apparent lack of correlation between the form of the electric field distribution and the level of magnetic disturbance.

Acknowledgments

The author is indebted to the principal and co-investigators for the OGO-6 experiment, Drs. T. L. Aggson and N. C. Maynard, respectively, for making these observations possible. The Explorer-33 magnetic field data made available through Dr. D. S. Colburn, NASA-Ames Research Center and the NASA National Space Science Data Center is gratefully acknowledged.

References

Aggson, T. L. and J. R. Bohse, World-wide ionospheric electric field patterns (Abstract: 53rd Annual AGU meeting), EOS, 53, 495, 1972.

Axford, W. I. and C. O. Hines, A unifying theory of high latitude geophysical phenomena and geomagnetic storms, Can. J. Phys., 39, 1433-1464, 1961.

Friis-Christensen, E., K. Lassen, J. Wilhjelm, J. M. Wilcox, W. Gonzalez, and D. S. Colburn, Critical component of the interplanetary magnetic field responsible for large geomagnetic effects in the polar cap, J. Geophys. Res., in press, 1972.

Heppner, J. P., Electric field variations during substorms: OGO-6 measurements, Planet. Space Sci., 20, in press, 1972a.

Heppner, J. P., Electric fields in the magnetosphere, Proc. of the Symposium on Critical Problems of Magnetospheric Physics, Madrid, Spain, May 1972, in press, 1972b.

Jørgensen, T. S., E. Friis-Christensen, and J. Wilhjelm, Interplanetary magnetic field direction and high-latitude ionospheric currents, J. Geophys. Res., 77, 1976-1977, 1972.

Mansurov, S. M., New evidence of a relationship between magnetic fields in space and on earth, Geomag. and Aeron., 9, 622-623, 1969.

Svalgaard, L., Sector structure of the interplanetary magnetic field and daily variation of the geomagnetic field at high latitudes, Geophys. Paper R-6, Danish Meteorol. Inst., Charlottenlund, 1968.

Wilhjelm, J. and E. Friis-Christensen, Electric fields and high-latitude zonal currents induced by merging of field lines, Planet. Space Sci., 20 (in press) 1972.

Figure Captions

Figure 1: Successive traverses across southern and northern high latitudes from two orbits of OGO-6 illustrating large asymmetries in the polar cap field distributions. The sign of E_x is in spacecraft coordinates which reverse relative to poleward, equatorward, and dawn-dusk directions in the two hemispheres.

Figure 2: Northern polar cap signature classification.

Figure 3: IP magnetic field and Kp values during cases of A and D and E signatures (northern polar cap).

Figure 4: IP magnetic field and Kp values during cases of B, C, and SC and RC signatures (northern polar cap).

Figure 5: IP magnetic field and Kp values during well defined cases of dawn-dusk asymmetry in the southern polar cap field.

Figure 6: IP magnetic field ϕ angle distributions for combined northern polar cap signatures and comparison with the southern polar cap.

Figure 7: To illustrate parallel and anti-parallel magnetospheric and IP magnetic fields for ϕ in the 90°-180° quadrant.

Figure 8: To explain the correlation between ϕ (or Y_{se}) and dayside polar magnetic activity found by Svalgaard (1968) and Mansurov (1969) in terms of asymmetric electric field distributions. Idealized for northern high latitudes. Ionospheric Hall currents flow in reverse direction of the convective flow.

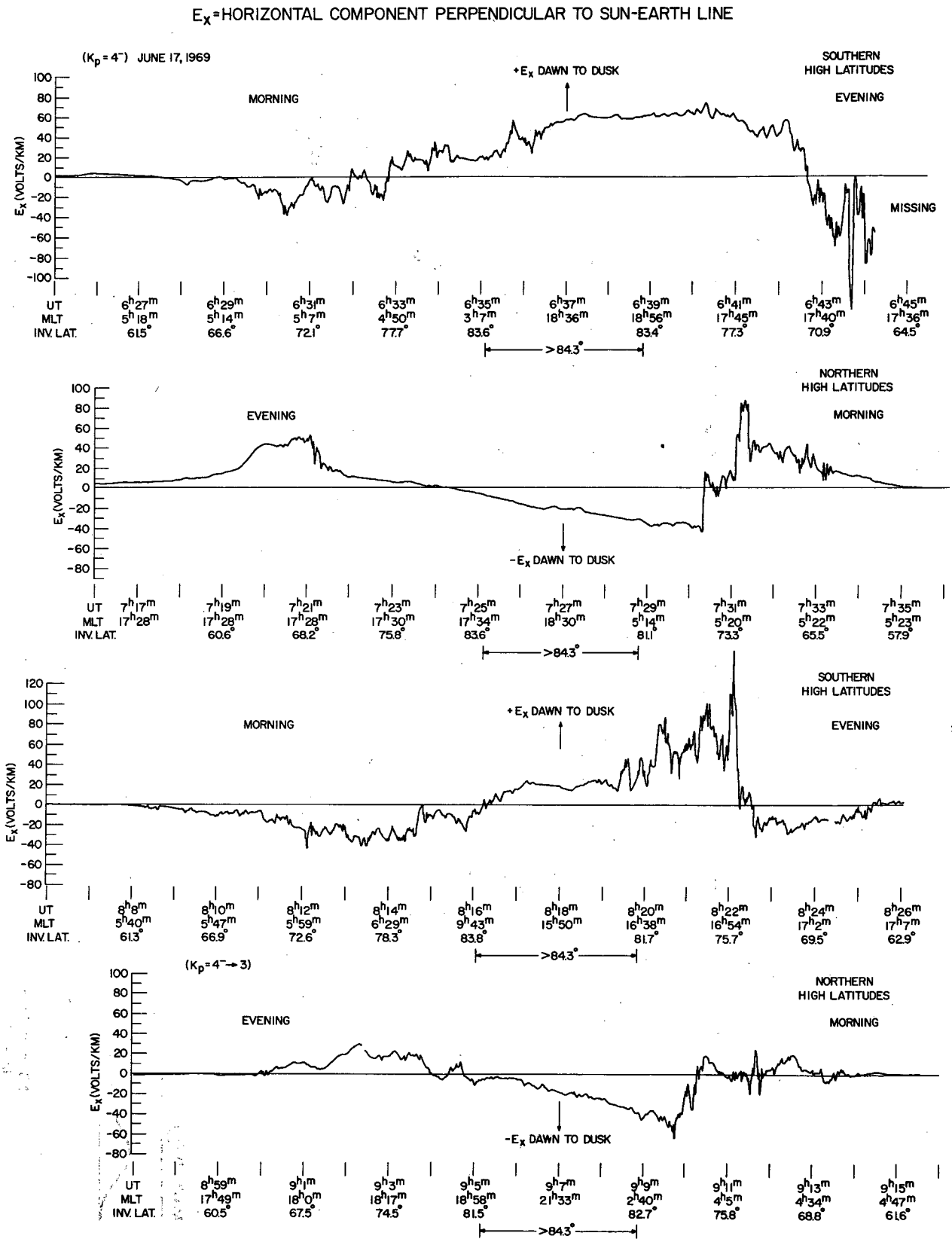
E_x=HORIZONTAL COMPONENT PERPENDICULAR TO SUN-EARTH LINE
(K_p=4⁻) JUNE 17, 1969
SOUTHERN HIGH LATITUDES
+E_x DAWN TO DUSK
MORNING
EVENING
MISSING
E_x (VOLTS/KM)
UT
MLT
INV. LAT.
>84.3°
NORTHERN HIGH LATITUDES
EVENING
MORNING
-E_x DAWN TO DUSK
SOUTHERN HIGH LATITUDES
+E_x DAWN TO DUSK
MORNING
EVENING
(K_p=4⁻→3)
NORTHERN HIGH LATITUDES
EVENING
MORNING
-E_x DAWN TO DUSK

Figure 1

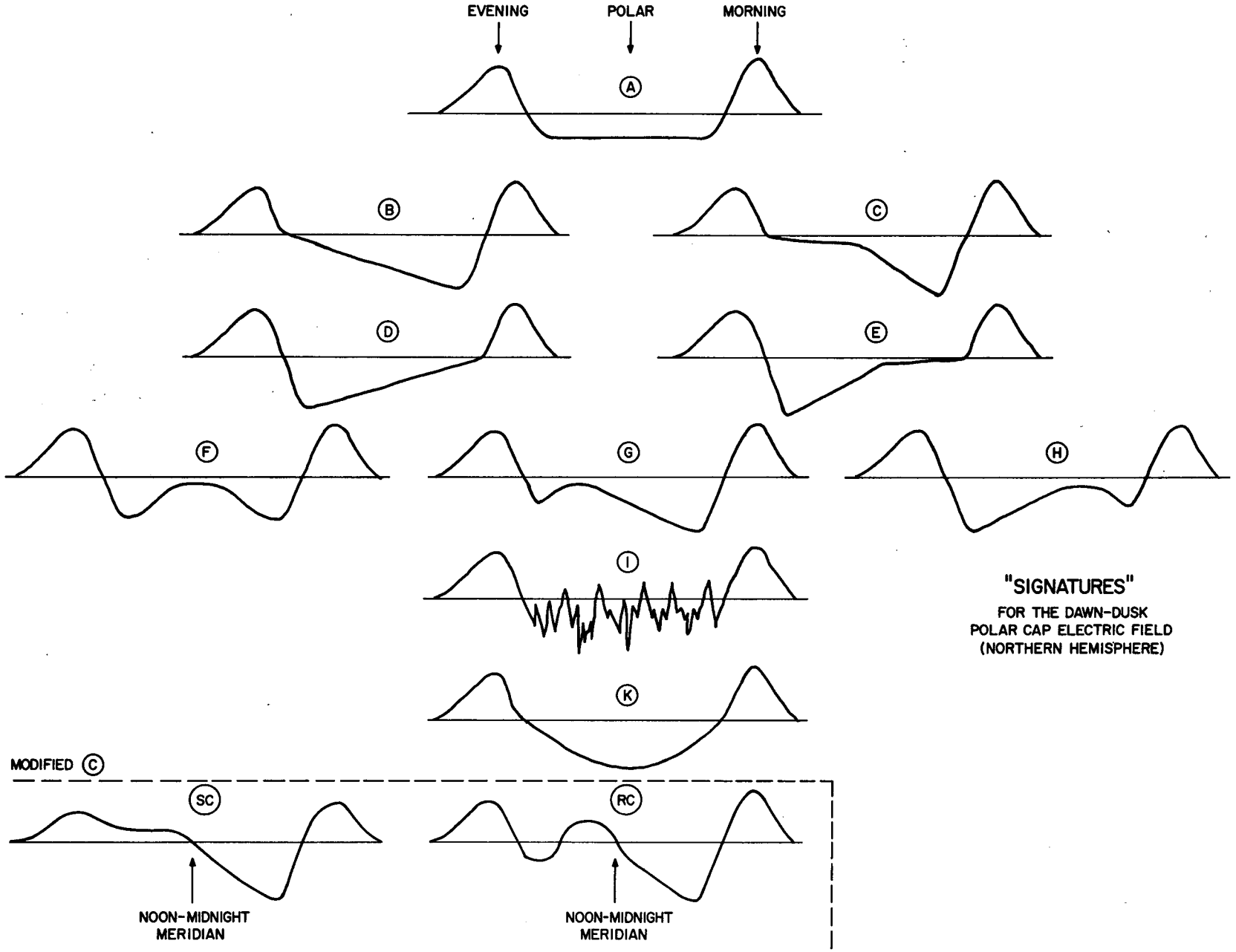
EVENING
POLAR
MORNING
A
B
C
D
E
F
G
H
I
K
"SIGNATURES"
FOR THE DAWN-DUSK
POLAR CAP ELECTRIC FIELD
(NORTHERN HEMISPHERE)
MODIFIED C
SC
RC
NOON-MIDNIGHT
MERIDIAN
NOON-MIDNIGHT
MERIDIAN

Figure 2

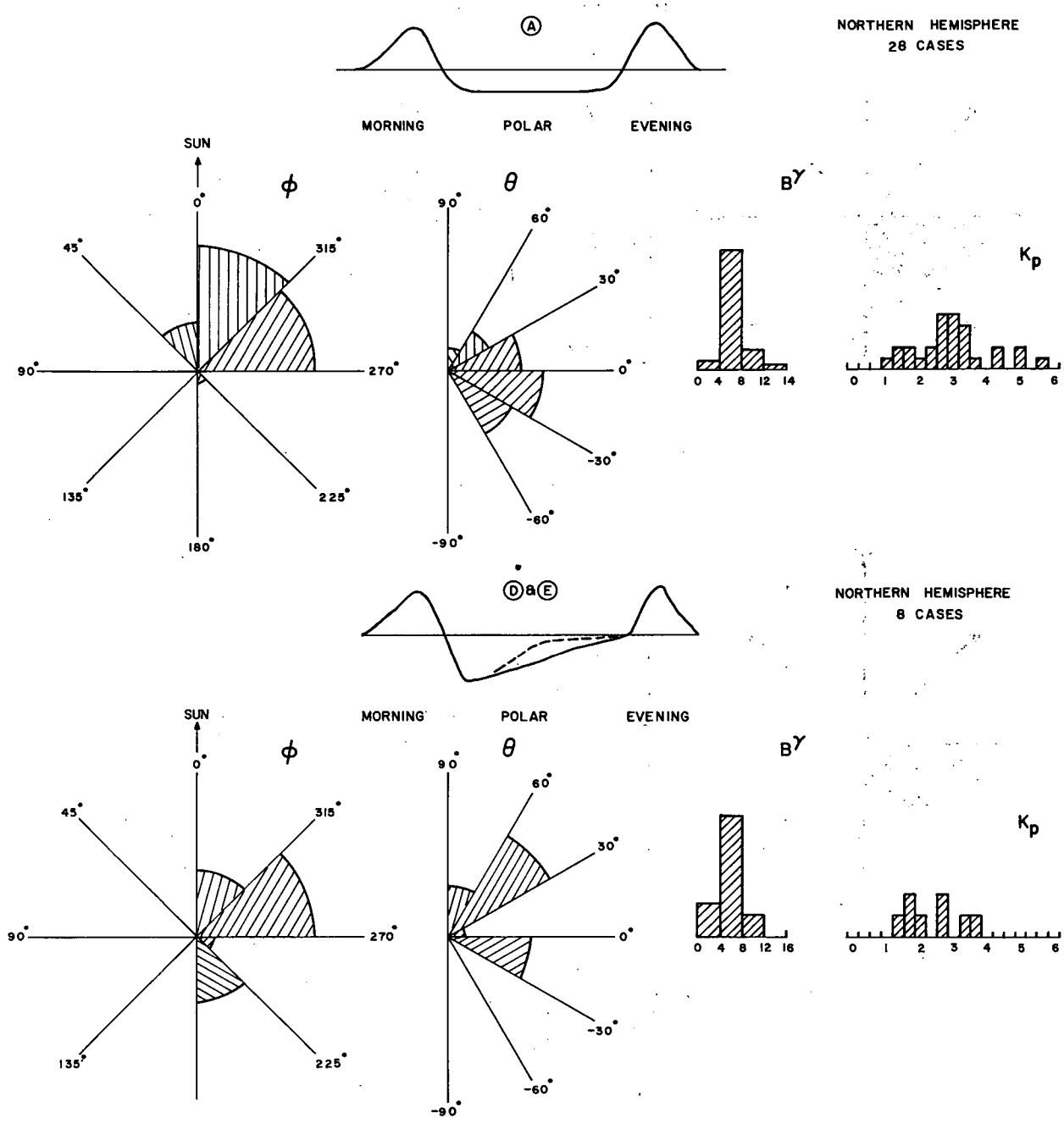
Ⓐ
NORTHERN HEMISPHERE
28 CASES
MORNING
POLAR
EVENING
SUN
ϕ
θ
B^γ
K_p
0°
45°
315°
90°
270°
135°
225°
180°
90°
60°
30°
0°
-30°
-60°
-90°
0 4 8 12 14
0 1 2 3 4 5 6
Ⓓ&Ⓔ
NORTHERN HEMISPHERE
8 CASES
MORNING
POLAR
EVENING
SUN
ϕ
θ
B^γ
K_p
0°
45°
315°
90°
270°
135°
225°
90°
60°
30°
0°
-30°
-60°
-90°
0 4 8 12 16
0 1 2 3 4 5 6

Figure 3

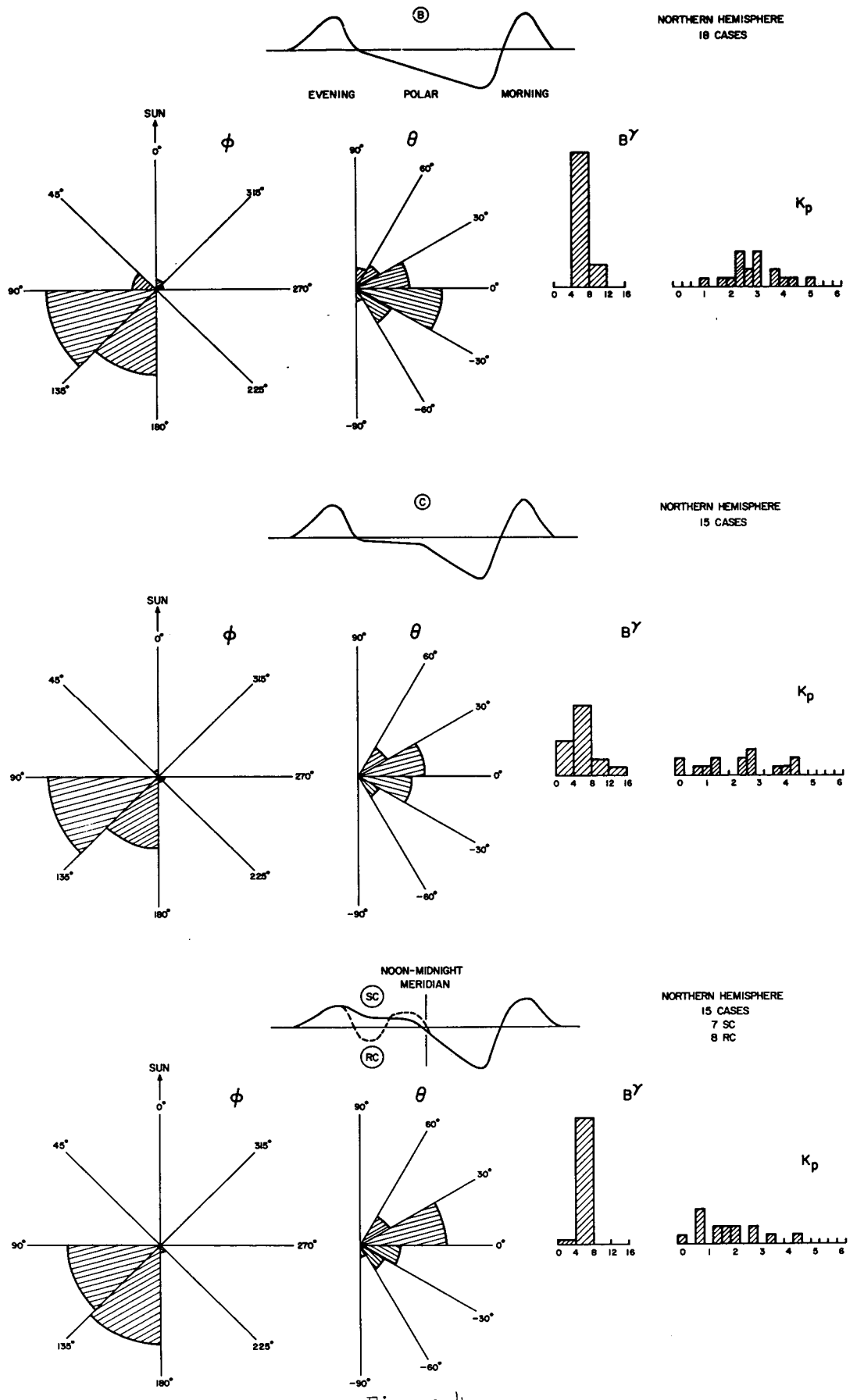
Ⓑ
NORTHERN HEMISPHERE
18 CASES
EVENING
POLAR
MORNING
SUN
0°
45°
315°
90°
270°
135°
225°
180°
ϕ
θ
90°
60°
30°
0°
-30°
-60°
-90°
B^Y
0 4 8 12 16
K_p
0 1 2 3 4 5 6
Ⓒ
NORTHERN HEMISPHERE
15 CASES
NOON-MIDNIGHT
MERIDIAN
SC
RC
NORTHERN HEMISPHERE
15 CASES
7 SC
8 RC

Figure 4

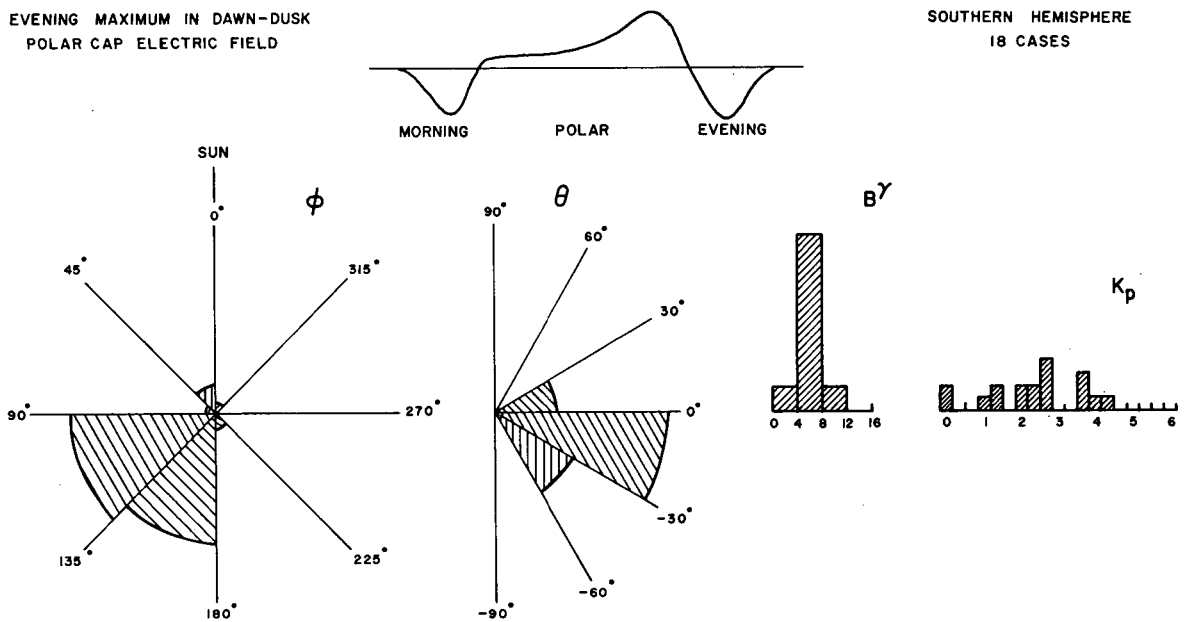
EVENING MAXIMUM IN DAWN–DUSK
POLAR CAP ELECTRIC FIELD
SOUTHERN HEMISPHERE
18 CASES
MORNING
POLAR
EVENING
SUN
0°
45°
315°
90°
270°
135°
225°
180°
ϕ
θ
90°
60°
30°
0°
-30°
-60°
-90°
B^Y
0 4 8 12 16
Kp
0 1 2 3 4 5 6
MORNING MAXIMUM IN DAWN–DUSK
POLAR CAP ELECTRIC FIELD
SOUTHERN HEMISPHERE
16 CASES
MORNING
POLAR
EVENING
0°
45°
315°
90°
270°
135°
225°
180°
ϕ
θ
90°
60°
30°
0°
-30°
-60
-90°
B^Y
0 4 8 12 16
Kp
0 1 2 3 4 5 6

Figure 5

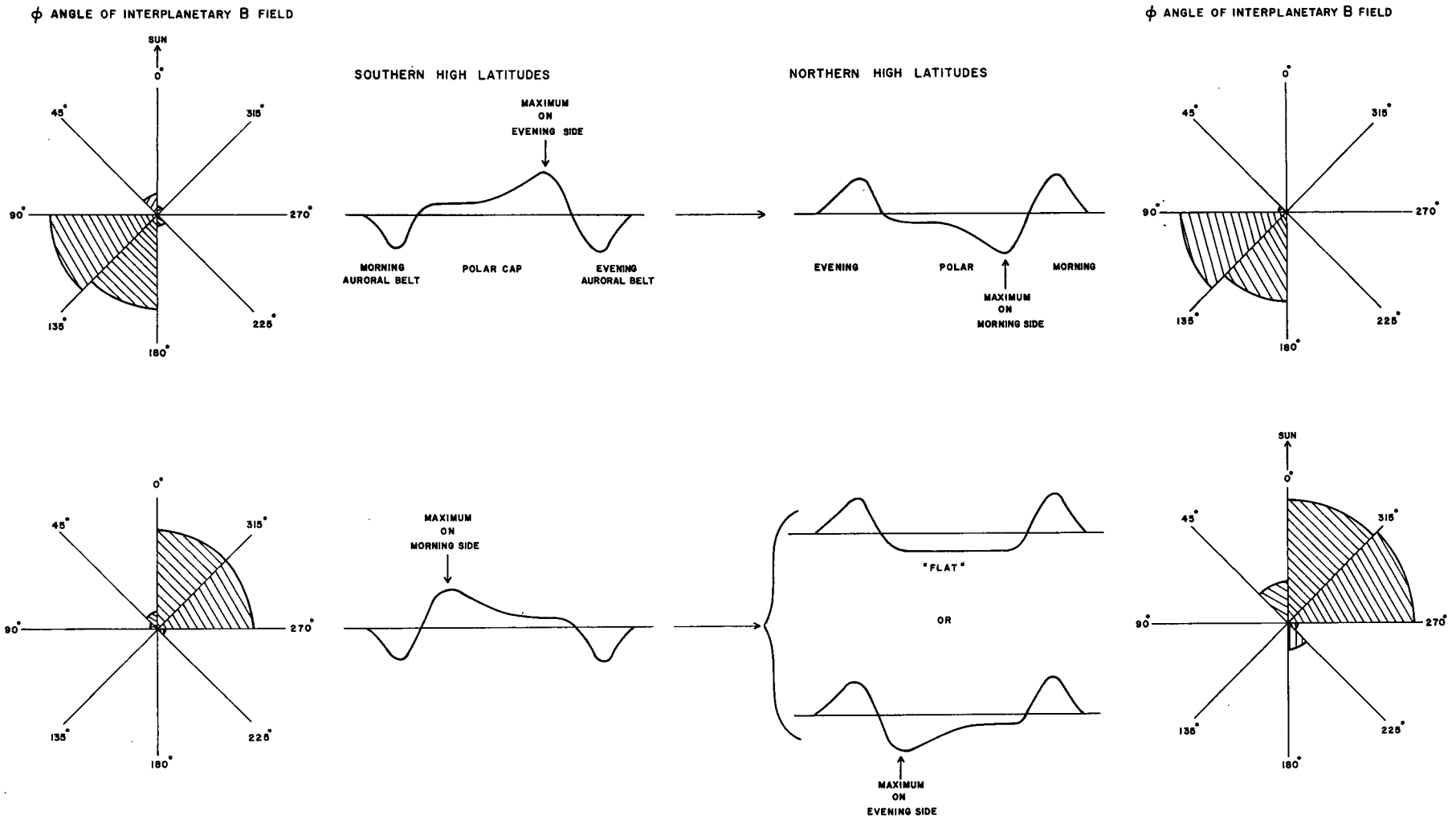
ANTI-CORRELATED DISTRIBUTION
OF THE
DAWN-DUSK ELECTRIC FIELD
ACROSS THE
SOUTHERN AND NORTHERN POLAR CAPS
ϕ ANGLE OF INTERPLANETARY B FIELD
SUN
0°
45°
315°
90°
270°
135°
225°
180°
SOUTHERN HIGH LATITUDES
MAXIMUM
ON
EVENING SIDE
MORNING
AURORAL BELT
POLAR CAP
EVENING
AURORAL BELT
NORTHERN HIGH LATITUDES
EVENING
POLAR
MORNING
MAXIMUM
ON
MORNING SIDE
ϕ ANGLE OF INTERPLANETARY B FIELD
MAXIMUM
ON
MORNING SIDE
"FLAT"
OR
MAXIMUM
ON
EVENING SIDE
SUN

Figure 6

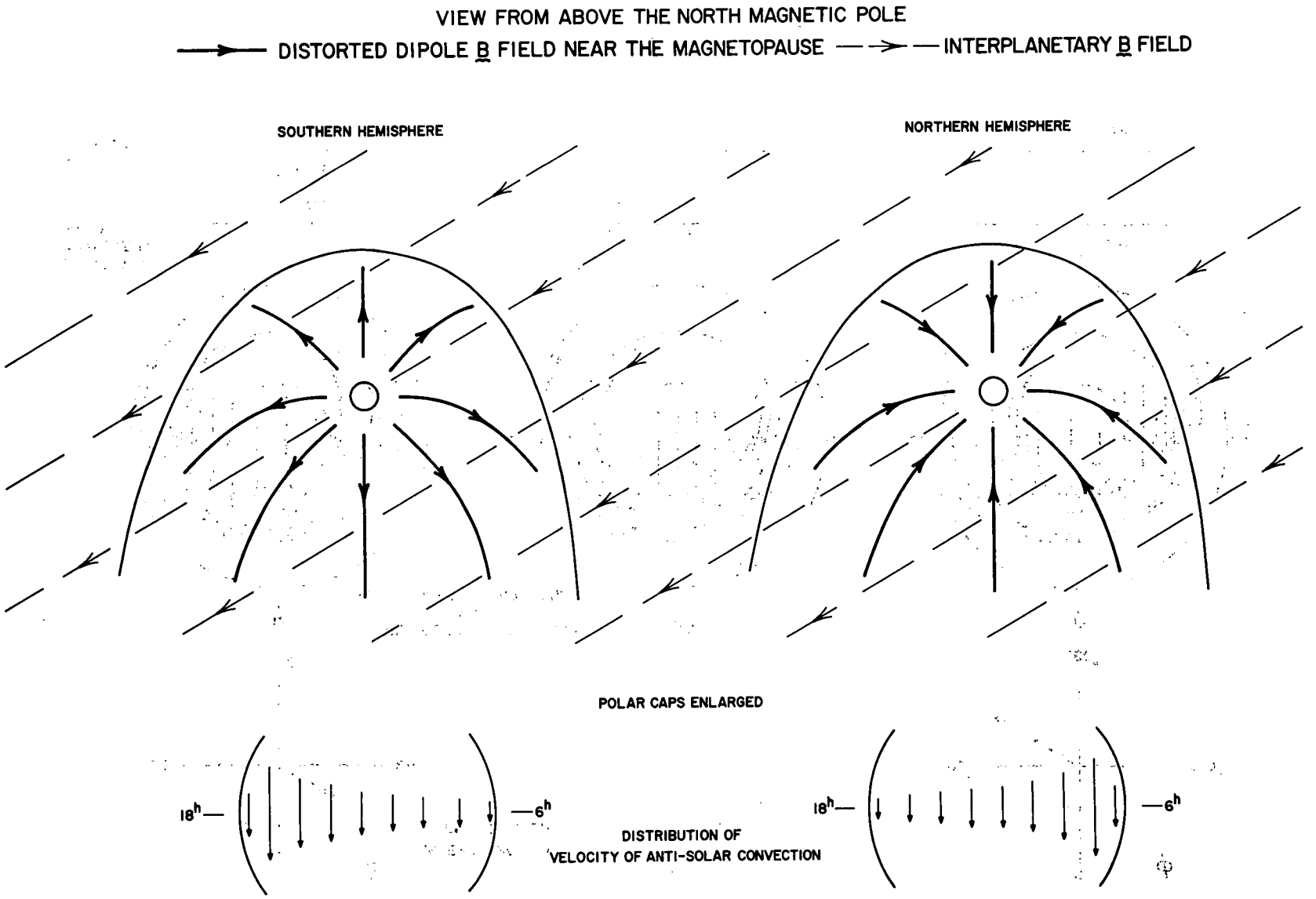
VIEW FROM ABOVE THE NORTH MAGNETIC POLE
DISTORTED DIPOLE B FIELD NEAR THE MAGNETOPAUSE
INTERPLANETARY B FIELD
SOUTHERN HEMISPHERE
NORTHERN HEMISPHERE
POLAR CAPS ENLARGED
18h
6h
18h
6h
DISTRIBUTION OF
VELOCITY OF ANTI-SOLAR CONVECTION

Figure 7

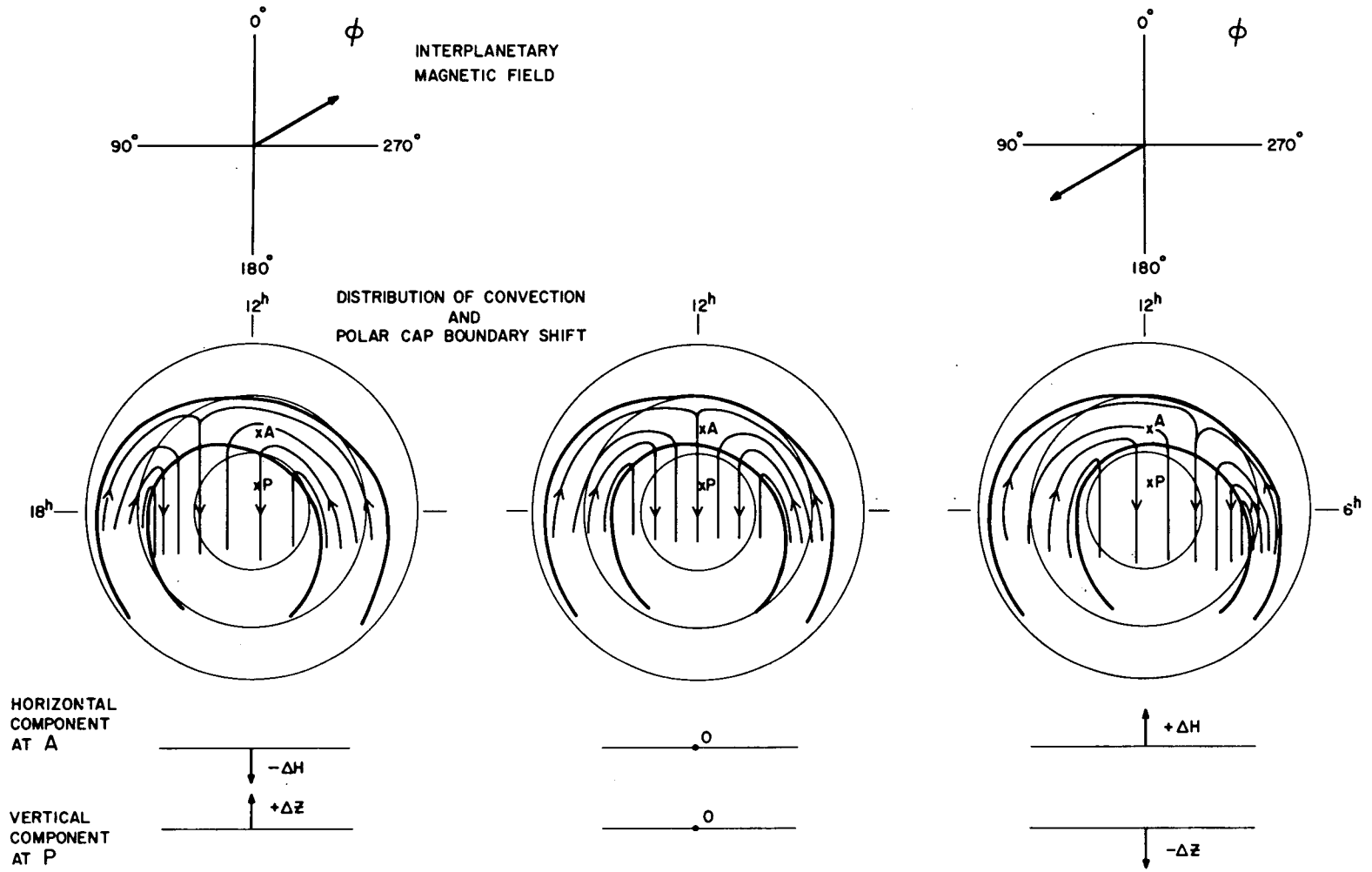

Figure 8

NASA–GSFC